Mechanics of Composite Materials, Vol. 47, No. 3, July, 2011 (Russian Original Vol. 47, No. 3, May-June, 2011)

A COMPARATIVE STUDY ON THE MECHANICAL AND BARRIER CHARACTERISTICS OF POLYIMIDE NANOCOMPOSITE FILMS FILLED WITH NANOPARTICLES OF PLANAR AND TUBULAR MORPHOLOGY

V. E. Yudin,[1*] J. U. Otaigbe,[2] S. I. Nazarenko,[2] W. D. Kim,[3] and E. N. Korytkova[4]

Keywords: *nanocomposites, polyimide, inorganic nanoparticles, mechanical properties, oxygen permeability*

Polyimide (PI) films based on poly(pyromellitic dianhydride-co-4,4'-oxydianiline) (PI-PM) were filled with different nanoparticles, such as organically modified montmorillonite (MMT), vapor-grown carbon nanofibers (VGCF), and silicate nanotubes (SNT) of different concentration.. Rheological measurements and structural investigations showed a relatively good dispersion of the nanoparticles in the PI matrix to an extent that depended on the type and morphology of the nanoparticles used. The mechanical (tensile modulus, strength, and deformation at break) and the barrier (oxygen permeability) properties of PI-PM nanocomposite films were investigated. The polyimide nanocomposites filled with SNT and tubular VGCF nanoparticles showed an increased tensile modulus with increasing volume concentration of the nanoparticles without a catastrophic decrease in the elongation at break. In addition, the MMT particles, chemically modified with 4,4'-bis-(4''-aminophenoxy)diphenylsulfone, significantly improved the barrier properties of the PI-PM films, which exceeded those of the nanocomposites filled with VGCF or SNT. The relative poor oxygen barrier and mechanical properties of the PI-PM/VGCF nanocomposite films are ascribed to the relative weak adhesion between the VGCF and the polyimide matrix, which was confirmed by scanning electron microscopy of the fracture surface of these films.

[1] Institute of Macromolecular Compounds, Russian Academy of Science, St. Petersburg, Russia
[2] School of Polymers and High Performance Materials, the University of Southern Mississippi, Hattiesburg, MS 39406, USA
[3] Kangwon National University, 1 Chungang, Samcheok, Ganwon, 245-711, Korea
[4] Institute of Silicate Chemistry, Russian Academy of Sciences, St. Petersburg, Russia
*Corresponding author; tel.: +7-812-323-5065; fax: +7-812-328-6869; e-mail: yudin@hq.macro.ru

Russian translation published in Mekhanika Kompozitnykh Materialov, Vol. 47, No. 3, pp. 485-496 , May-June, 2011. Original article submitted November 26, 2010.

1. Introduction

The creation of hybrid organic-inorganic nanocomposites in which the size of the inorganic phase does not exceed 100 nm is one of the most promising ways for obtaining new polymeric materials with improved properties. In this context, it is worthy of note that nanocomposites prepared from organic (polymer) and inorganic (nanoparticle) constituents have been reported to present materials with a new hierarchical structure at the molecular and supermolecular levels and with properties different from the simple sum of those of their constituents.

In the last decade, a number of publications on polymer nanocomposites have focused on nanocomposites reinforced with carbon nanotubes or nanofibers and silicate nanoparticles such as montmorillonite (MMT), a natural laminated silicate with a layer thickness of at least 1 nm, as evidenced by a number of review articles, e.g., [1, 2]. Polymer/MMT nanocomposites belong to a relatively new class of reinforced polymer nanocomposites, containing uniformly dispersed MMT nanoparticles in a polymer matrix. Such nanocomposites are reported to have various practical advantages due to their relatively high mechanical and barrier properties, as well as a good fire-resistance [3, 4].

In contrast to the polymer/MMT nanocomposites mentioned in the literature, a high loading of up to 10 vol.% silicate nanotubes [5, 6] or carbon nanofibers [7] in polyimide films with a rather high elongation at break can be achieved [8]. These new polyimide nanocomposites provide the possibility of significantly increasing the concentration of nanoparticles in polyimide without reducing the elongation at break (or ductility) of the polymer matrix. Therefore, these nanocomposites may be useful in new applications that require an optimal resistance to the thermal oxidation and good gas/liquid barrier properties.

A special interest in developing new polyimide (PI)-based nanocomposites is caused by their expected excellent heat resistance, chemical stability, and superior electric properties [9]. For example, it has been reported that PI nanocomposites can exhibit an increased elastic modulus and strength, a high heat distortion temperature, a decreased thermal expansion coefficient, a reduced gas permeability, and an increased solvent resistance relative to the corresponding parameters of the pure polymer [1, 2]. The aim of the current study is to compare the mechanical and barrier properties of PI-type nanocomposite films filled with lamellar (MMT) and tubular (carbon or silicate) nanoparticles and to clear up their efficiency in improving the performance (e.g., the mechanical properties and oxygen permeability) of pure polyimide films for potential new applications where the conventional polymer nanocomposites are unsuitable.

2. Experimental

2.1. Organic treatment of MMT. The natural montmorillonite clay Na-MMT [Cloisite®Na+, cation exchange capacity (CEC) 92.6 meq/100g] was obtained from Southern Clay Products, Inc. The density of the particles was about 2.6 g/cm^3. The hydrochloric acid (concentration 36.5%) and 4,4′-*bis*-(4′′-aminophenoxy) diphenylsulfone (BAPS) were obtained from Fisher Chemical and Wakayama Seika Kogyo Co., Ltd. in Japan, respectively. The Na-MMT was organically modified with BAPS ammonium salts by using the method described in detail in [8]. The modified MMT particles used in the current study are hereinafter referred to as MMT-BAPS.

2.2. Carbon nanofibers and silicate nanotubes. The vapor-grown carbon nanofibers (VGCF), which were graphitized at 2800°C, were supplied by Showa Denko K. K. Japan. They had an average diameter and length of 150 and 10-20 μm, respectively, and a density of 2 g/cm^3. The silicate nanotubes (SNT) with a chrysotile-type structure were synthesized by a hydrothermal method, facilitated by using high-pressure autoclaves, as described elsewhere [10, 11]. The SNT density was 2.5 g/cm^3. The average length and outer diameter of the SNT particles were 85.2 and 14.3 nm, respectively, giving an average aspect ratio of 6. The inner diameter of the tubular SNT nanoparticles was approximately 4 nm. In contrast to the MMT-BAPS nanoparticles already described, the as-received VGCF and SNT were incorporated into the PI matrix without any surface treatment.

2.3. Polyimide matrices. The poly(amic acid) (PAA) of poly(pyromellitic dianhydride-co-4,4′-oxydianiline) (PM) was supplied by Sigma-Aldrich. The PAA-PM was a 15.0 wt.% solution in N-methyl-2-pyrrolidone (NMP). The PI films (30-40 mm thick) were prepared by casting the PAA-PM on soda lime glass plates and subsequent drying in an oven at 80°C for

12 h in an air atmosphere. The imidization was achieved by placing the films in an air oven for curing at 100°C for 1 h, 200°C for 1 h, 300°C for 1 h, and 350°C for 30 min. After complete imidization, the films were removed from the plates by soaking in water. The density of the PI-type film prepared, hereinafter referred to as PI-PM, was 1.42 g/cm^3.

An oligoimide (OI) based on 1,3-*bis*-(3,3′,4,4′-dicarboxyphenoxy)benzene and BAPS and endcapped with phthalic anhydride was synthesized following the procedure described in [12]. Note that OI with the following chemical structure was used as a model material for evaluating the rheological behavior of polyimide matrix filled with nanoparticles:

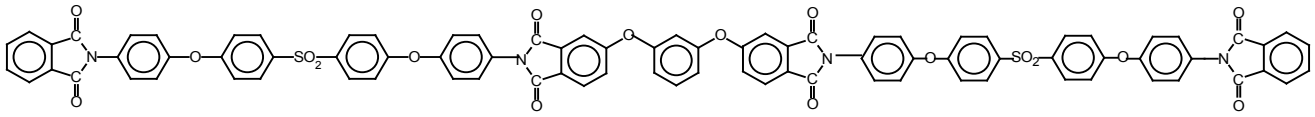

The number-average molecular weight (M_n) and the weight-average molecular weight (M_w) of the OI were 3609 and 11553 g/mol, respectively, according to the data of size-exclusion chromatography [12].

2.4. Processing of nanocomposites. PI-PM nanocomposite films with different concentrations of nanoparticles (MMT-BAPS, SNT, or VGCF) were prepared by adding a desired amount of the nanoparticles to the NMP. The resulting suspension was homogenized with the aid of an ultrasonic mixer (22 ± 0.1 kHz, average sonic power 45 W) for one hour. The sonicated suspension was poured into a three-neck round-bottom flask equipped with a mechanical stirrer, a nitrogen gas inlet, and a tubular drying outlet filled with calcium sulfate. After stirring the nanoparticle solution for 10 min, the PAA-PM was added to the nanoparticle suspension, and stirring of the mixture was continued for additional 60 min until a constant viscosity was obtained. The solid content of the nanoparticle/PAA-PM in the NMP was 10 wt.%. Thin (30-40-mm-thick) PI-PM nanocomposite films with various nanoparticle weight concentrations *wt* were prepared from the nanoparticle/PAA-PM solution, as already described above for the case of pure (unfilled) PI-PM films. From the known densities of the materials used (1.42 g/cm^3 for PI-PM, 2.6 g/cm^3 for MMT-BAPS, 2.5 g/cm^3 for SNT, and 2 g/cm^3 for VGCF), the corresponding volume concentrations *V* of nanoparticles in the polyimide nanocomposites were estimated using the formula

$$V = \frac{1}{1+\frac{\rho_1}{\rho_2}\left(\frac{1}{wt}-1\right)} \quad , \tag{1}$$

where ρ_1 is the density of particles and ρ_2 is the density of polymer matrix.

A simple solution mixing method was employed to prepare a mixture of NMP solution of OI with nanoparticles (MMT-BAPS, VGCF, or SNT). First, the nanoparticles were dispersed in NMP by using an ultrasonic mixer (40 kHz, average sonic power 45W) for one hour. Various amounts of the nanoparticles were used to obtain the final OI/nanoparticle mixtures, containing 3 to 20 wt.% of the respective particles. Then, an NMP solution of OI (20 wt.%) was added to the nanoparticle/NMP dispersion, and the combined mixture was stirred with a magnetic blender for five hours. The resulting NMP dispersion of OI with nanoparticles was poured on a Teflon®-coated metal substrate, which was subsequently exposed to 100˚C for one hour, 200˚C for one hour, and 280˚C for 0.5 hours to completely remove the NMP solvent, which was monitored by a TGA. The Teflon® coating made it easy to collect the OI/nanoparticle blends in the form of a powder. The powder samples were used to prepare test specimens for rheological measurements, which are described in the next section.

2.5. Measurements. A strain-controlled dynamic rheometer ARES® from TA Instruments was used to measure the dynamic and steady-shear viscosity of OI/nanoparticle blends in the cone and plate configuration following standard procedures. The diameter of the plate was 25 mm, and the cone angle was 0.1 rad. Nitrogen was used as the heating gas to control the temperature. The OI/nanoparticle powder samples were compacted into disks 25 mm in diameter at room temperature by using a compression molding machine. The disk was then placed between the plates of the rheometer, which were preheated to a desired temperature.

The tensile stress-strain properties of the PI-PM-based nanocomposite films were determined by using a tensile testing machine (Alliance RT/10, MTS systems Co., Ltd.) according to the standard ASTM D882-95 method. Specimens with a gage length of 50 mm and width of 5 mm were used. An abrasive paper was placed between the specimen and fixture surface to

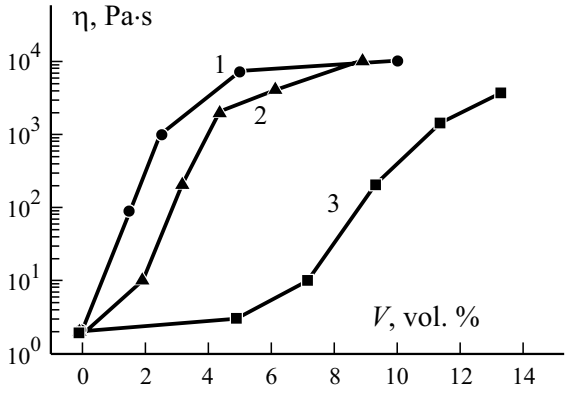

Fig. 1. The complex viscosity η vs. the volume concentration V of MMT-BAPS (1), VGCF (2), and SNT (3) nanoparticles in the oligoimide OI at T = 260°C, ω = 1 rad/s, and ε = 1%.

prevent slippage. Ten tests were conducted for each sample, and the average results are reported in this paper. The morphology of fracture surfaces of PI film samples filled with VGCF and SNT nanoparticles was observed using a high-resolution scanning electron microscope (HRSEM, FEI Sirion).

The oxygen barrier of the nanocomposites was measured at 25°C and a 1-atm partial oxygen pressure difference by means of a commercially manufactured diffusion apparatus OX-TRAN® 2/21 ML (MOCON). The film specimens were covered with an aluminum foil having a 50-cm^2 circular hole. Prior to testing, the ~40-mm-thick PI films were conditioned in nitrogen inside the apparatus to remove the traces of atmospheric oxygen and water vapor. The method of measuring the coefficient of oxygen permeability was described earlier in [6] for PI-PM films filled with STN.

3. RESULTS AND DISCUSSION

3.1. Rheology of oligoimides filled with nanoparticles. As reported previously [5-8], OI/nanoparticle nanocomposites can be used as model systems for investigating the flow and deformation conditions for an optimal dispersion of the particles in PI used in the current study. Figure 1 shows the complex viscosity (frequency ω = 1 rad/s and strain ε = 1%) against the concentration of nanofillers (MMT-BAPS, VGCF, and SNT) for the OI nanocomposites prepared as described in the experimental section. The viscosities of the nanocomposites were estimated at 260°C — the temperature corresponding to the Newtonian fluid state of the OIs. The figure shows a significant increase in the viscosity (~3 decades) of OI/MMT-BAPS, OI/VGCF, and OI/SNT nanocomposites with ~2 vol.% MMT-BAPS, ~3 vol.% VGCF, and ~10 vol.% SNT nanofillers, respectively.

To evaluate the feasibility of a homogeneous dispersion of the nanoparticles in the polyimide matrix, we used a rheological method which was found to be effective for characterizing the dispersibility of lamellar and tubular particles in a polymer [5]. Homogenous dispersions of nanoparticles in polymers should exhibit a time-dependent rheological behavior (i.e., thixotropy), which is characteristic of percolation-type networks at some nanoparticle concentrations. Generally, it is possible to estimate this percolation threshold R_p theoretically [13] by using the formula

$$R_p = 0.6/r,$$

for a cylinder and

$$R_p = 1.27/r,$$

for an ellipsoid, where r = L/d is the aspect ratio, L is the length of the cylinder or the diameter of the ellipsoid, and d is the diameter of the cylinder or thickness of the ellipsoid.

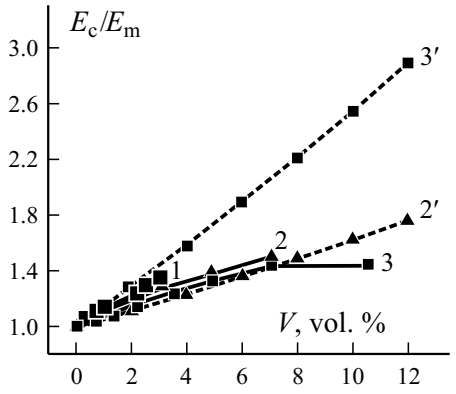

Fig. 2. The normalized tensile moduli E_c/E_m of PI-PM nanocomposite films as functions of volume concentration V of MMT-BAPS (1), SNT (2, 2′), and VGCF (3, 3′) nanoparticles: (———) — experimental; (– – –) — calculation by Eq. (1).

The preceding equations and the average aspect ratios of ~20 for VGCF and ~6 for SNT can be used to estimate the percolation threshold R_p, which was found to be ~ 3 and ~ 10 vol.%, respectively. Assuming, according to [3], an average diameter (lateral dimension) of ~ 200 nm and a thickness of ~ 1 nm for the MMT particles, the percolation threshold for them was estimated at 0.64 vol.%. These data were found to be close to those obtained from rheological measurements. Therefore, it can be concluded that the nanoparticles have been relatively well dispersed during preparation of the nanocomposites. Since the method of OI/nanoparticle preparation is similar to that used for the PI-PM/nanoparticles films (see Sect. 2.4.), it is reasonable to expect that the nanoparticles should also be well dispersed in the films.

3.2. Mechanical properties of PI nanocomposite films. The tensile moduli (Young's moduli) E_c of the PI-PM-based nanocomposite films at room temperature are summarized in Fig. 2, where the ordinate is E_c normalized to the modulus E_m = 3.0 GPa of the PI-PM matrix. Note that the tensile moduli were determined at strains of 0.3 to 0.5%. To estimate the tensile modulus E_c of the PI-PM films filled with nanotubes, we used the model of a lamina with in-plane randomly oriented fibers, according to which [14-16]

$$\frac{E_c}{E_m} = \frac{3}{8}\left(\frac{1+2(l_f/d_f)\eta_L V_f}{1-\eta_L V_f}\right) + \frac{5}{8}\left(\frac{1+2\eta_T V_f}{1-\eta_T V_f}\right), \tag{1}$$

where

$$\eta_L = \frac{(E_f/E_m)-1}{(E_f/E_m)+2(l_f/d_f)}, \quad \eta_T = \frac{(E_f/E_m)-1}{(E_f/E_m)+2}. \tag{2}$$

In Eqs. (1) and (2), E_m and E_f are the matrix and filler moduli, l_f and d_f are the length and diameter of nanotubes, and V_f is the volume fraction of nanotubes in the nanocomposite.

In the corresponding calculations, the following values of the elastic moduli and aspect ratios of nanofibers found in the literature were taken: E_f(SNT) = 160 GPa [17], E_f(VGCF) = 500 GPa [18], l_f/d_f(SNT) = 6 [19], and l_f/d_f(VGCF) = 20 [14]. The experimental data for the PI-PM films filled with SNT were found to be consistent with calculated (theoretical) values (Fig. 2). In contrast to the polyimide/SNT nanocomposites, the PI-PM films filled with VGCF gave theoretical results significantly higher than the corresponding experimental data. This discrepancy can be ascribed to the rather weak stress transfer between the polymer matrix and VGCF nanofibers, leading to debonding and sliding at the interfaces between the nanofibers and the polymer matrix. This hypothesis was supported by the SEM of the fracture surface of the polyimide/VGCF nanocomposite films, which revealed evidence for the pull-out of significant lengths of nanofibers from the matrix (Fig. 3a). Compared with the polyimide/VGCF nanocomposite, the polyimide/SNT nanocomposite showed a relatively good adhesion between the

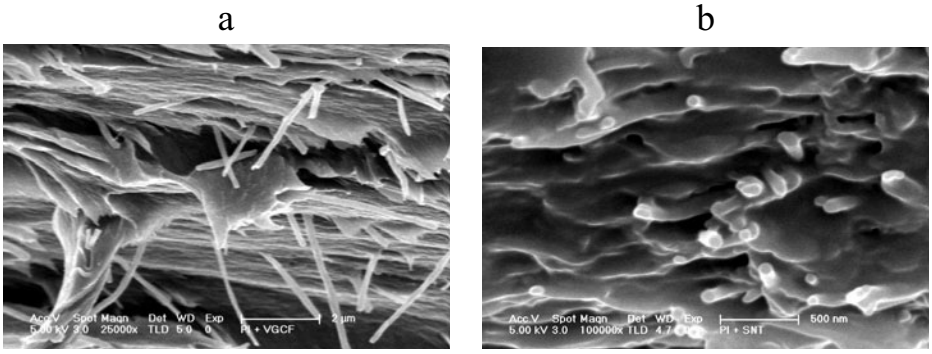

Fig. 3. SEM of the fracture surface of PI-PM/VGCF (a) and PI-PM/SNT (b) nanocomposite films.

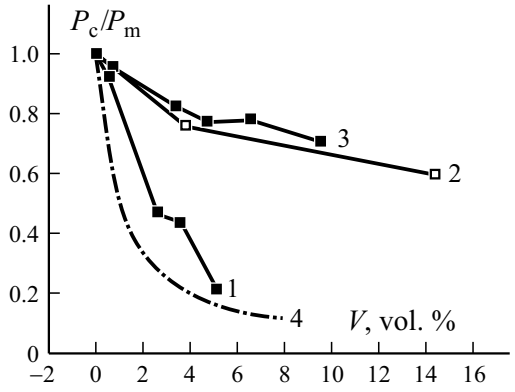

Fig. 4. The relative oxygen permeability P_c/P_m as a function of volume fraction V of MMT-BAPS (1), VGCF (2), and SNT (3) nanoparticles in PI-PM nanocomposite films: (———) — experiment; (— · — · —) — calculation by Eq. (3) for MMT (L = 200 nm and d = 1 nm).

nanotubes and matrix (see Fig. 3b), which could be explained by the presence of hydroxyl groups on the nanotube surface. The preceding results suggest that the discrepancy between the observed tensile moduli and their theoretical predictions is primarily caused by the rather poor adhesion between VGCF and the polyimide matrix. As indicated in [20], the mechanical properties (the tensile modulus in particular) of PI-PM/VGCF nanocomposite films can be significantly improved by using pretreated VGCF with an effective surface modification in addition to homogeneously dispersing the nanoparticles in the polymer matrix. The surface modification of VGCF prior to their incorporation into the polyimide matrix is believed to improve the transfer of stress in the nanocomposite from the polymer to the relatively stiff and strong VGCF.

3.3. Barrier properties of PI nanocomposite films. The oxygen permeability of PI-PM films filled with MMT-BAPS, VGCF, or SNT was estimated by using the procedure described in Sect. 2.5. The coefficient of oxygen permeability P_m for a PI-PM control film, 1.26 cc cm/m^2/day/atm, was found to be in excellent agreement with the value 1.28 cc cm/m^2/day/atm previously reported in the literature for the same polyimide system [21]. The relative permeability of the PI-PM films filled with MMT-BAPS platelets was predicted using Nielsen's equation [22]

$$P_c / P_m = 1/[1 + (L/2d)V_f], \tag{3}$$

where V_f is the volume fraction of particles, and L and d are their length and thickness. Assuming an average diameter (lateral dimension) of ~200 nm and thickness of ~1 nm for the MMT particles, obtained from the literature [3], we calculated the

relative permeabilities of the films. The values obtained are indicated in Fig. 4, which shows that the experimental relative permeability of the PI-PM/MMT-BAPS nanocomposite films is comparable to that given by Eq. (3). However, the experimental values are higher, which can be explained by the partial aggregation of MMT particles, as reported in [8, 12] and also follows from experimental data (see Sect. 3.1). Overall, the results for the relative permeability show that the incorporation of MMT particles (modified by using the thermally stable ammonium salt) into polyimide can significantly decrease the oxygen permeability of polyimide films, making them potentially useful in a number of new applications, such as anticorrosion coatings.

In contrast to the polyimide/MMT, the incorporation of SNT and VGCF with a relatively high aspect ratio (≥ 20) into the polyimide matrix did not lead to a significant improvement in the barrier properties of the PI-PM films, as depicted in Fig. 4. This behavior of the polyimide/VGCF nanocomposite films is surprising, because the aspect ratio of VGCF is at least 20 (i.e., four times greater than that of SNT). However, according to the expression (expansion approximation) derived by Fredrickson and Shaqfeh for a low volume fraction of rods [23], the relative permeability of PI-PM films filled with VGCF with a high aspect ratio should be lower than that of PI-PM films filled with SNT. Nevertheless, the experimental values of barrier properties of the PI-PM/VGCF and PI-PM/SNT were practically the same, indicating that the increased aspect ratio of tubular nanoparticles does not lead to an improvement in the barrier properties of polyimide nancomposites containing these nanoparticles. One plausible explanation of this experimental fact is the rather low adhesion between VGCF and PI-PM, as already mentioned (see Fig. 3b), which can lead to the formation of channels for a significant diffusion of oxygen through the film thickness. It is reasonable to expect that the surface modification of VGCF can improve both the barrier and the mechanical properties of PI-PM/VGCF, but increasing the aspect ratio of SNT-type particles can improve the barrier properties of PI-PM/SNT nanocomposite films. This is a matter for future investigations.

4. CONCLUSIONS

MMT organically modified with a thermally stable amine (BAPS) can be incorporated into a polyimide matrix at elevated temperatures to improve its mechanical and barrier properties. The incorporation of 5 vol.% MMT-BAPS particles in PI-PM films can decrease the oxygen permeability of these films more than five times. In contrast, the incorporation of tubular nanoparticles, such as SNT with a low aspect ratio (~ 6) or VGCF with a relatively high aspect ratio (~20), in a polyimide matrix does not significantly improve the barrier properties (oxygen permeability) of PI-PM nanocomposite films. However, the tubular nanoparticles can be incorporated into the PI-PM matrix at relatively high volume fractions (up to 14 vol.%) to yield nanocomposites with relatively high modulus and elongation at break. The relative poor improvement of the mechanical (tensile modulus) and barrier (oxygen permeability) properties of PI-PM/VGCF is possibly caused by the rather poor adhesion between VGCF and the polyimide matrix. This study suggests that a better understanding of the relationships between the processing, structure, and properties of polyimide nanocomposites containing nanofillers of different geometry and dimensions is needed to afford new polymeric materials with optimal properties for applications in high-temperature and aggressive environments.

REFERENCES

1. H. Fischer, “Polymer nanocomposites: From fundamental research to specific applications,” Mater. Sci. Eng., **23**, 763-772 (2003).
2. F. Hussain, M. Hojjati, M. Okamoto, and R. E. Gorga, “Polymer-matrix nanocomposites, processing, manufacturing, and application: An overview,” J. Compos. Mater., **40**, 1511-1575 (2006).
3. S. Ray and M. Okamoto, “Polymer/layered silicate nanocomposites: A review from preparation to processing,” Progr. Polym. Sci., **28**, 1539-1641 (2003).
4. Q. Zeng, A. Yu, G. Lu, and D. Paul, “Clay-based polymer nanocomposites: Research and commercial development,” J. Nanosci. Nanotechn., **5**, 1574-1592 (2005).

5. V. E. Yudin, J. U. Otaigbe, V. M. Svetlichnyi, E. N. Korytkova, O. V. Almjasheva, and V. V. Gusarov, "Effects of nanofiller morphology and aspect ratio on the rheo-mechanical properties of polyimide nanocomposites," eXPRESS Polym. Lett., **2**, 485-493 (2008).
6. V. E. Yudin, J. U. Otaigbe, S. V. Gladchenko, B. G. Olson, S. I. Nazarenko, E. N. Korytkova, and V. V. Gusarov, "New polyimide nanocomposites based on silicate type nanotubes: Dispersion, processing and properties," Polymer, **48**, 1306-1315 (2007).
7. V. E. Yudin, J. U. Otaigbe, L. T. Drzal, and V. M. Svetlichnyi, "Novel semicrystalline thermoplastic R-BAPB type polyimide matrix reinforced by graphite nanoplatelets and carbon nanoparticles," Adv. Compos. Lett., **15**, 137-143 (2006).
8. K. Takashi, V. E. Yudin, J. U. Otaigbe, and V. M. Svetlichnyi, "Compatibilized polyimide (R-BAPS)/BAPS-modified clay nanocomposites with improved dispersion and properties," Polymer, **48**, 7130-7138 (2007).
9. M. I. Bessonov, M. M. Koton, V. V. Kudryavtsev, and L. A. Laius, Polyimides — Thermally Stable Polymers, Plenum Publ. Corp., New York (1987).
10. E. N. Korytkova, A. V. Maslov, L. N. Pivovarova, I. A. Drozdova, and V. V. Gusarov, "Formation of $Mg_3Si_2O_5(OH)_4$ nanotubes under hydrothermal conditions," Glass Phys. Chem., **30**, 51-55 (2004).
11. E. N. Korytkova, A. V. Maslov, L. N. Pivovarova, Y. V. Polegotchenkova, V. F. Povinich, and V. V. Gusarov, "Formation of $Mg_3Si_2O_5(OH)_4$-$Ni_3Si_2O_5(OH)_4$ nanotubes under high temperature and pressure," Inorgan. Mater., **41**, 1-7 (2005).
12. V. E. Yudin, G. Divoux, J. U. Otaigbe, and V. M. Svetlichnyi, "Synthesis and rheological properties of oligoimide/montmorillonite nanocomposites," Polymer, **46**, 10866-10872 (2005).
13. E. Garboczi, K. Snyder, J. Douglas, and M. Thorpe, "Geometrical percolation threshold of overlapping ellipsoids," Phys. Rev. E, **52**, 819-828 (1995).
14. T. Ogasawara, Y. Ishida, and T. Ishikava, "Properties of vapor-grown carbon nanofiber/phenylethynyl terminated polyimide composite," Adv. Compos. Mater., **13**, 215-226 (2004).
15. D. Qian, E. C. Dickey, R. Andrews, and T. Rantell, "Load transfer and deformation mechanisms in carbon nanotube-polystyrene composites," Appl. Phys. Lett., **76**, 2868-2870 (2000).
16. P. K. Mallick, Fiber-Reinforced Composites, Marcel Dekker, New York (1993).
17. S. Piperno, I. Kaplan-Ashiri, S. R. Cohen, R. Popovitz-Biro, H. D. Wagner, R. Tenne, E. Foresti, I. G. Lesci, and N. Roveri, "Characterization of geoinspired and synthetic chrysotile nanotubes by atomic force microscopy and transmission electron microscopy," Adv. Funct. Mater., **17**, 3332-3338 (2007).
18. R. L. Jacobsen, T. M. Tritt, J. R. Guth, A. C. Ehrlich, and D. J. Gillespie, "Mechanical properties of vapor-grown carbon fibers," Carbon, **33**, 1217-1221 (1995).
19. B. G. Olson, J. J. Decker, S. I. Nazarenko, V. E. Yudin, J. U. Otaigbe, E. N. Korytkova, and V. V. Gusarov, "Aggregation of synthetic chrysotile nanotubes in the bulk and in solution probed by nitrogen adsorption and viscosity measurements," J. Phys. Chem.: Part C, **112**, 12943-12950 (2008).
20. X. Chen, K. Yoon, C. Burger, I. Sics, D. Fang, B. S. Hsiao, and B. Chu, "In-situ x-ray scattering studies of a unique toughening mechanism in surface-modified carbon nanofiber/UHMWPE nanocomposite films," Macromolecules, **38**, 3883-3893 (2005).
21. S. A. Stern, Y. Mi, H. Yamamoto, and A. K. St. Clair, "Structure/permeability relationships of polyimide membranes: Applications to the separation of gas mixtures," J. Polym. Sci., Part B, **27**, 1887-1909 (1989).
22. L. E. Nielsen, "Models for the permeability of filled polymer systems," J. Macromol. Sci., Part A, **1**, 929-942 (1967).
23. G. H. Fredrickson and E. S. G. Shaqfeh, "Heat and mass transport in composites of aligned slender fibers," Phys. Fluids A: Fluid Dynamics, **1**, 3-20 (1989).